

Calibrating Test Sections for Calibration of Aerodynamic Probes

by
F. Kreitmeier

Summary:

As part of an experimental investigation of free jet test sections for calibration of aerodynamic probes some axisymmetric nozzles have been tested.

In the higher subsonic region a considerable probe - shaft influence was observed. The suitability of subsonic test sections ($Ma \leq 1$) using convergent nozzles has been demonstrated. For the supersonic range ($1 < Ma < 1.6$) test sections obtained with a ventilated and a convergent-divergent nozzle were found to be unsuitable.

1. INTRODUCTION

In the technique of flow measurements probes indicating "indirectly" are frequently used. The main feature of these particular probes is that a calibration is required to indicate the relation between the measurement and the flow variables.

There was a requirement for a uniform free jet test section in the technically important range of Ma 0.2 to 1.6.

For the calibration of these test sections probes permitting "direct" flow measurement should be used.

2. NOZZLE CONTOURS

Fig. 1 shows the contours of nozzles used for subsonic flow. The first nozzle shown on this graph, called "subsonic nozzle ϕ 80" has a throat diameter of 80 mm.

The second one called "subsonic nozzle ϕ 153.5" has a throat diameter of 153.5 mm.

The converging region of these nozzles is contoured according to WILLE [1]. The second slightly divergent region is for achieving uniform discharge flow conditions.

Fig. 2 shows the contours of nozzles used for supersonic flow.

The first one, called "supersonic nozzle ϕ 80/ perforated" is a composition of the "subsonic nozzle ϕ 80" and a perforated tube. The philosophy of this nozzle is to get an expansion of the flow as a result of ventilation through the perforated wall. Whenever the pressure ratio is higher than critical supersonic expansion occurs.

The second one called "supersonic nozzle ϕ 80/ contoured" has a throat diameter of 80 mm. It is an ordinary LAVAL nozzle. The subsonic part of it is contoured like the "subsonic nozzle ϕ 80". The supersonic part is defined according to FOELSCH [2]. The nominal discharge Mach number is 1.6.

3. TEST FACILITY AND EXPERIMENTAL TECHNIQUES

Fig. 3 shows the main parts and dimensions of the test facility.

The following quantities were measured: (s. Fig. 3)

- the independent flow variables \hat{p}_0 and \hat{T}_0 within the settling chamber and the ambient pressure \hat{p} .
- the dependent flow variables p_0 and p in the test section.

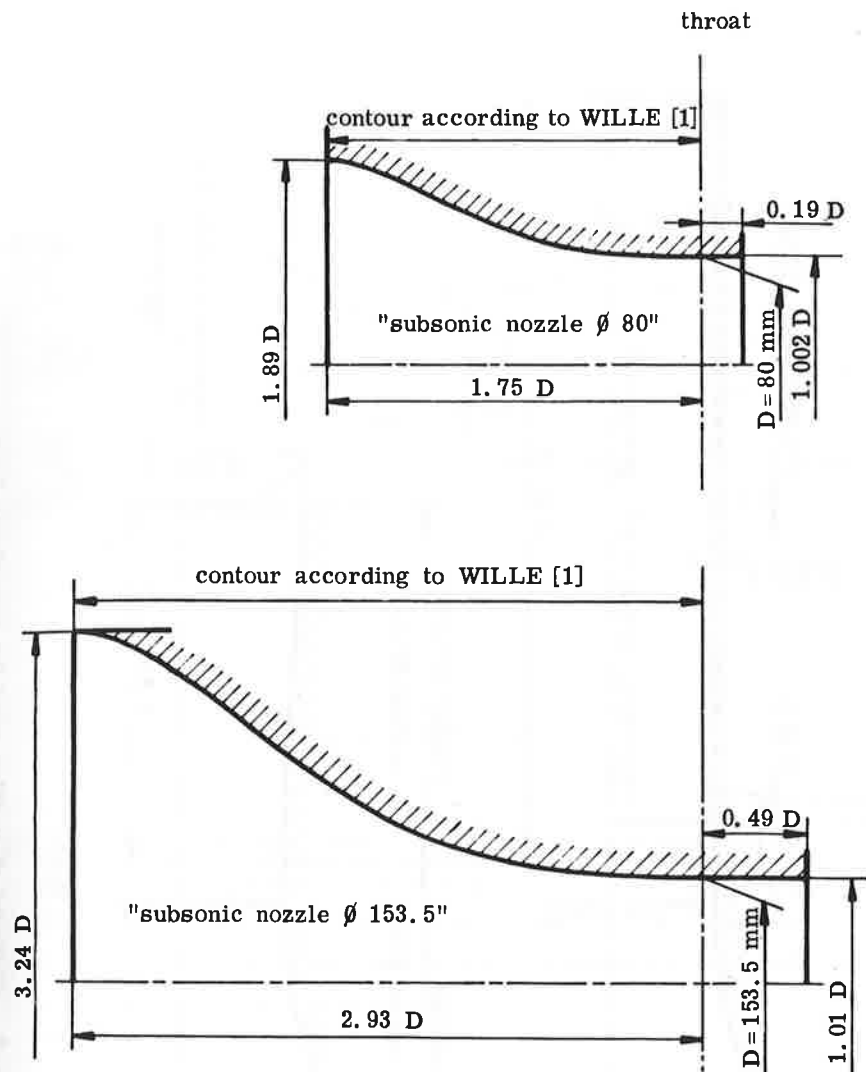


Fig. 1 Contours of nozzles used for subsonic flow

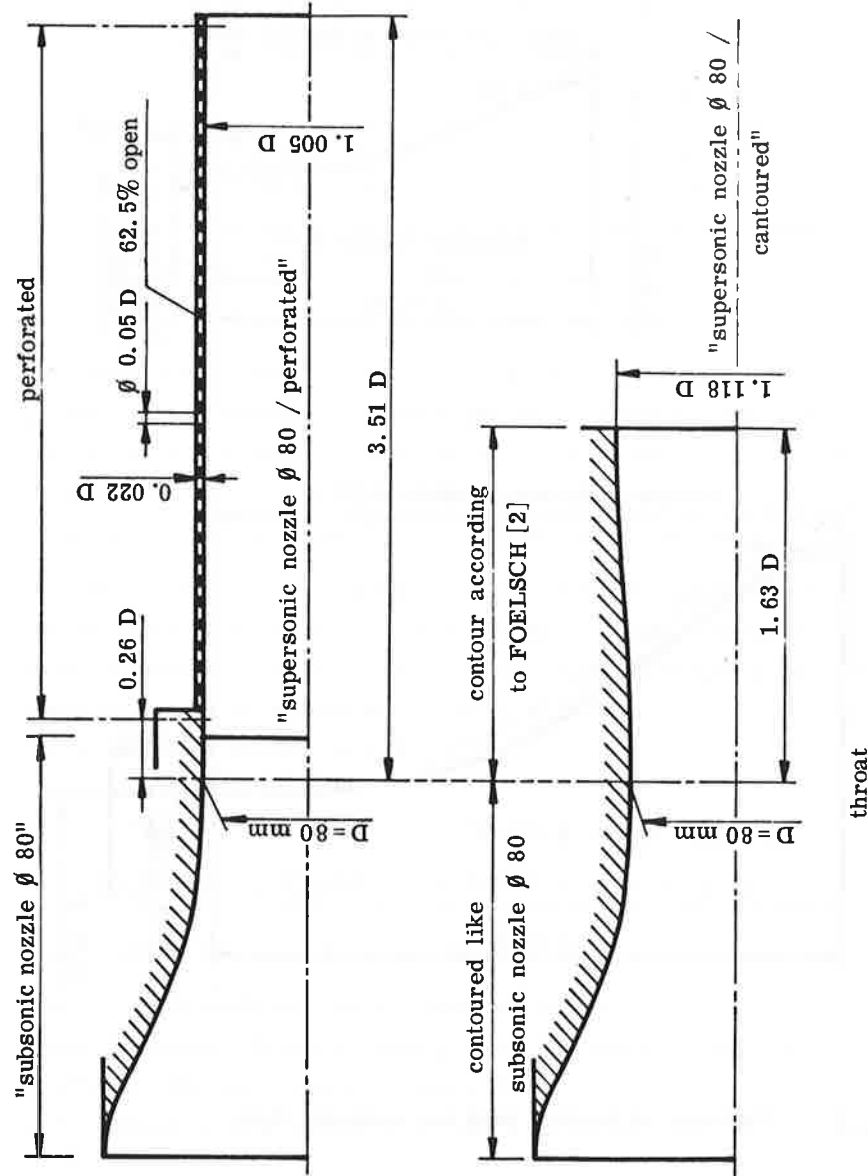


Fig. 2 Contours of nozzles used for supersonic flow

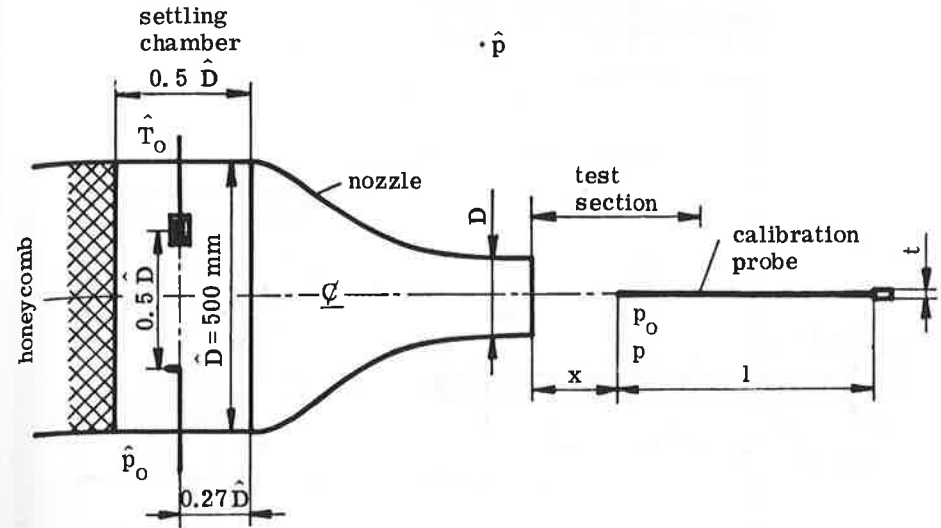


Fig. 3 Test facility

Fig. 4 shows the probes used for calibration of test sections. The probes have a reference diameter of 2.5 mm. For the supersonic region a special static pressure probe is used. It also indicates correctly in the subsonic region. 3 different distances and 2 different thicknesses of the shaft were used.

4. DATA REDUCTION

Fig. 5 shows the flow variables in an enthalpy-entropy diagram. The functional dependence is indicated. Especially the form with dimensionless parameters is of interest. Definitions of these parameters are given.

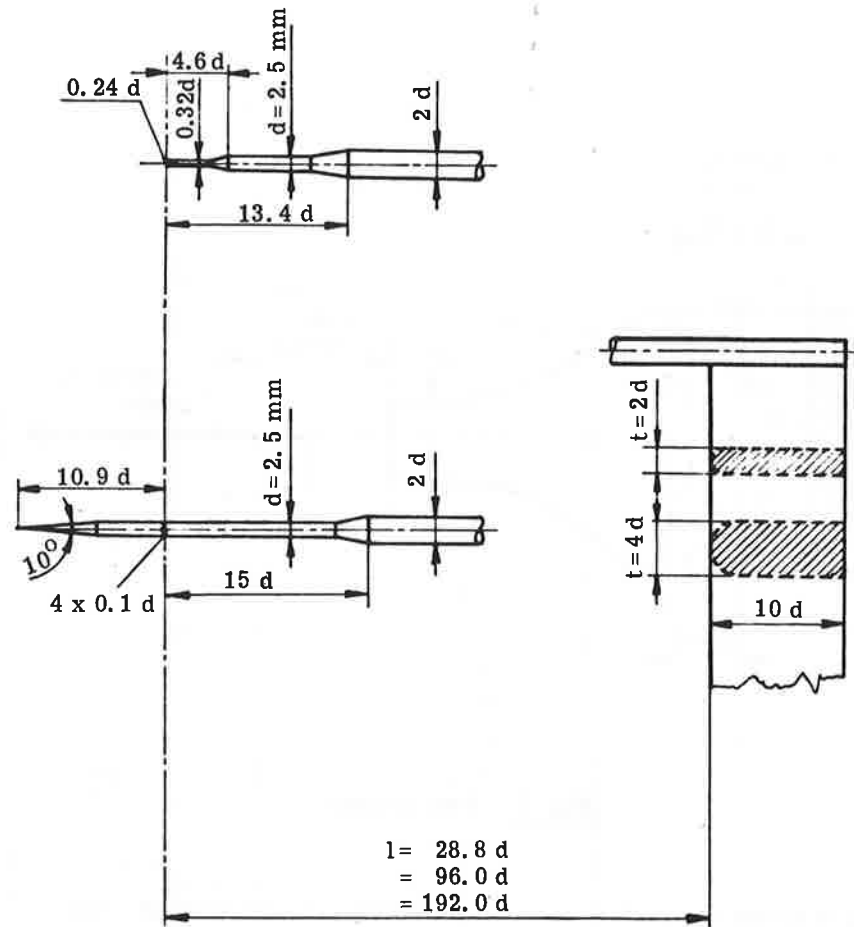
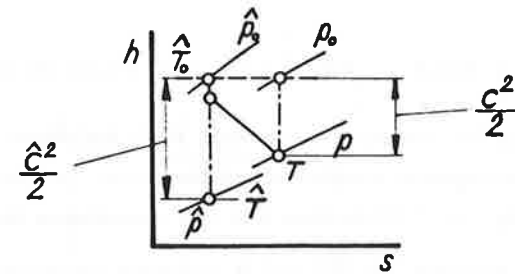


Fig. 4 Probes used for calibration of test sections



$$\rho_o, p = f(\text{geometry}, \hat{\rho}_o, \hat{T}_o, \hat{p}, \text{medium})$$

$$\left. \begin{array}{l} Re_D, Ma \\ \text{or} \\ C_p, C_p \end{array} \right\} = f(\text{geometric parameters}, \hat{Re}_D, \hat{Ma}, \hat{k})$$

$$x/D; l/t; A_s/A = 2t/\pi D$$

$$\hat{Re}_D = \frac{\hat{c} \cdot D}{\nu(\hat{p}, \hat{T})}$$

$$\hat{Ma} = \hat{c} / a(\hat{T})$$

$$Re_D = \frac{c \cdot D}{\nu(p, T)}$$

$$Ma = c / a(T)$$

$$C_p = \frac{p - \hat{p}}{\hat{p}_o - \hat{p}}$$

$$C_{p_o} = \frac{\rho_o - \hat{\rho}_o}{\hat{\rho}_o - \hat{\rho}}$$

Fig. 5 Data reduction

5. RESULTS

5.1 Probe-Shaft / Flow Interference Effects

Fig. 6 shows for the subsonic nozzle ϕ 80 the dependence of the static pressure discrepancy coefficient on the probe geometry. The first diagram for $\hat{Ma} = 0.6$ illustrates that the dependence is very small.

The second diagram for $\hat{Ma} = 0.8$ indicates an astonishing strong dependence. With increasing As/A the influence is reduced.

The third diagram for $\hat{Ma} = 1$ shows a strong dependence too but of smaller magnitude.

5.2 Measured Flow Characteristics of Test Sections

Fig. 7 gives for the subsonic nozzles the dependence of total - and static pressure discrepancy coefficients on the ideal Mach and Reynolds number.

The first plot shows the results for the subsonic nozzle ϕ 80, the second one the same for the subsonic nozzle ϕ 153,5. Remarkable is, that in the last case boundary layer effects and therefore total pressure losses are evident in the centre of the test section.

Fig. 8 shows for the perforated supersonic nozzle the dependence of the total - and static pressure discrepancy coefficients on the ideal Mach and Reynolds number. Striking are the great total pressure losses and the irregular static pressure variation.

Fig. 9 suggests for the same nozzle the total and static pressure discrepancy coefficients and the real Ma number along the axis. The total pressure decreases very rapidly and increases with the distance from the throat. The static pressure and the real Mach number vary irregularly.

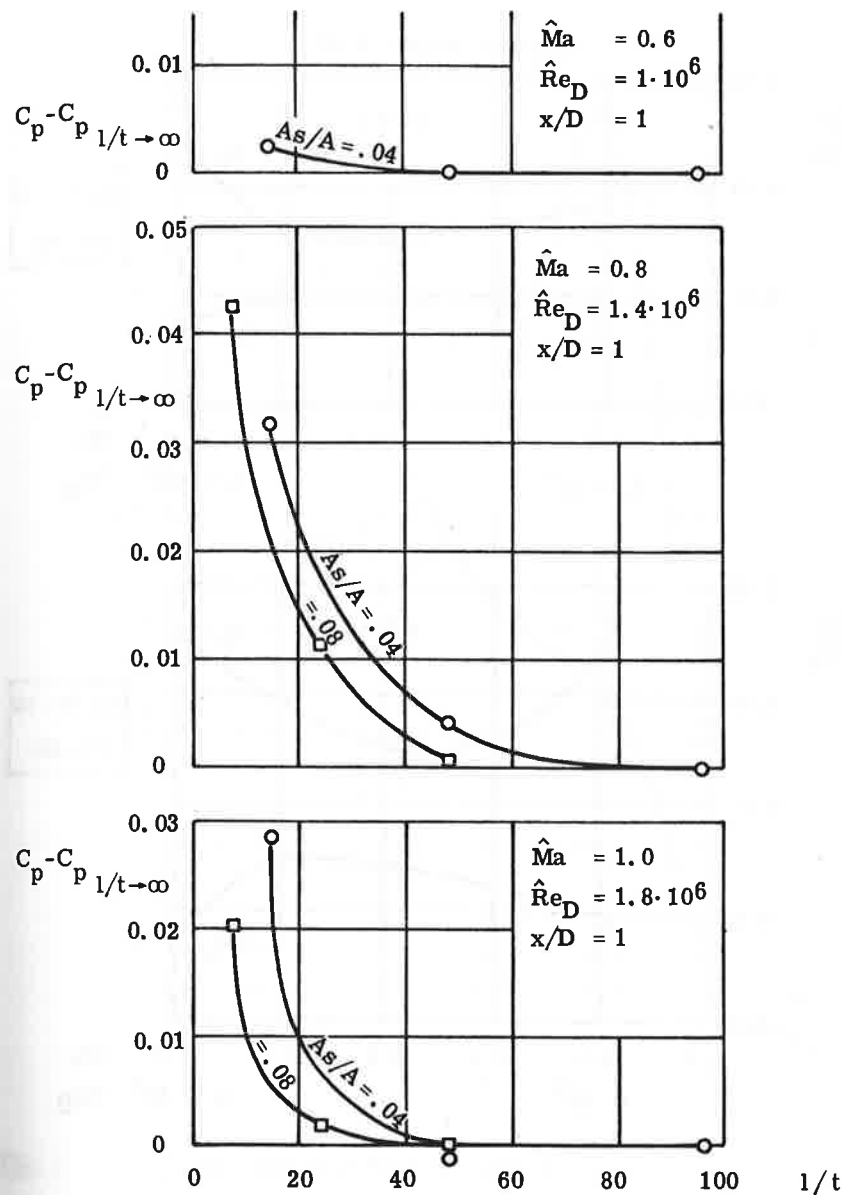


Fig. 6

Subsonic nozzle ϕ 80

Dependence of static pressure discrepancy coefficients on the probe geometry

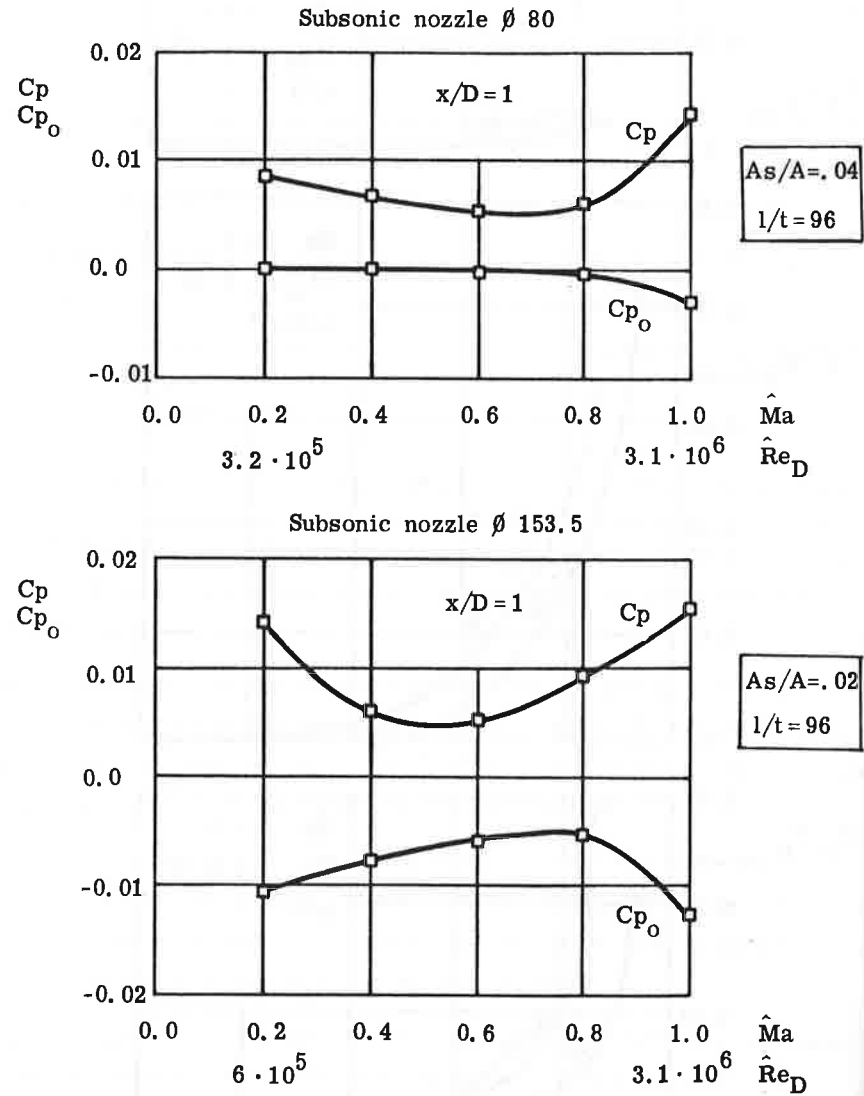


Fig. 7 Subsonic nozzles
 Dependence of total- and static pressure discrepancy coefficients on the ideal Mach and Reynolds number

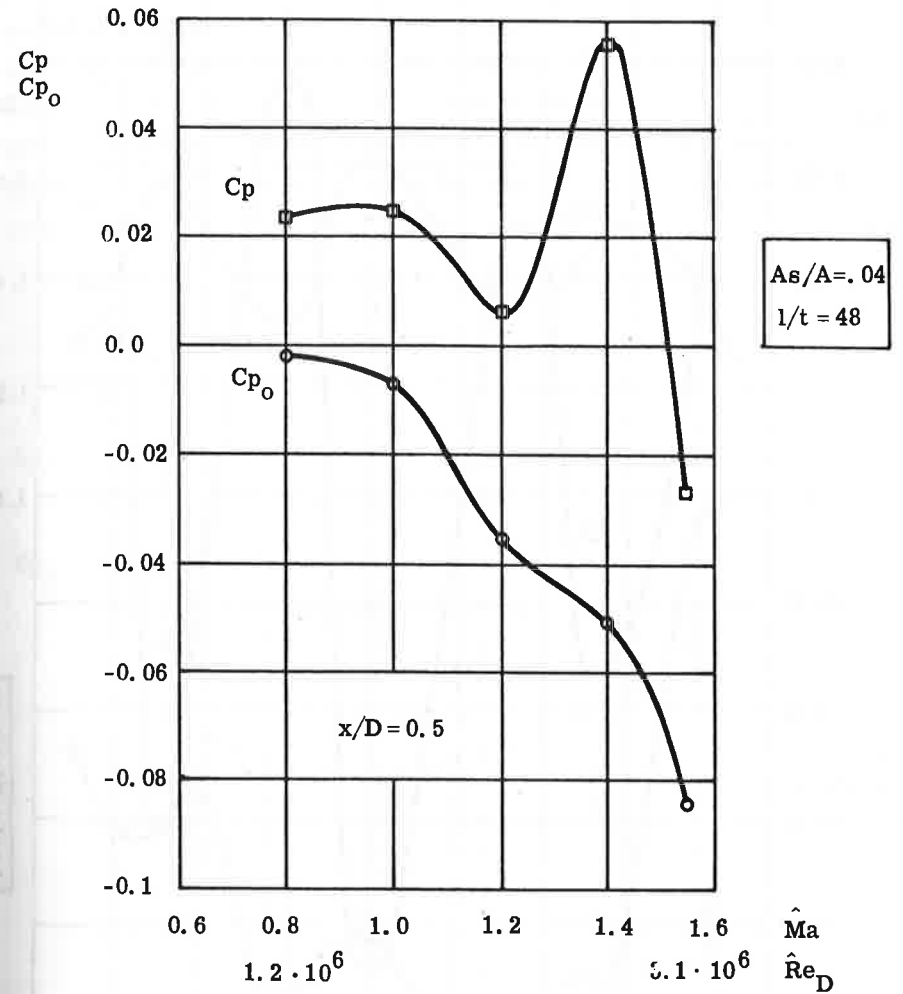


Fig. 8 Supersonic nozzle ø 80 / perforated
 Dependence of total- and static pressure discrepancy coefficients on the ideal Mach and Reynolds number

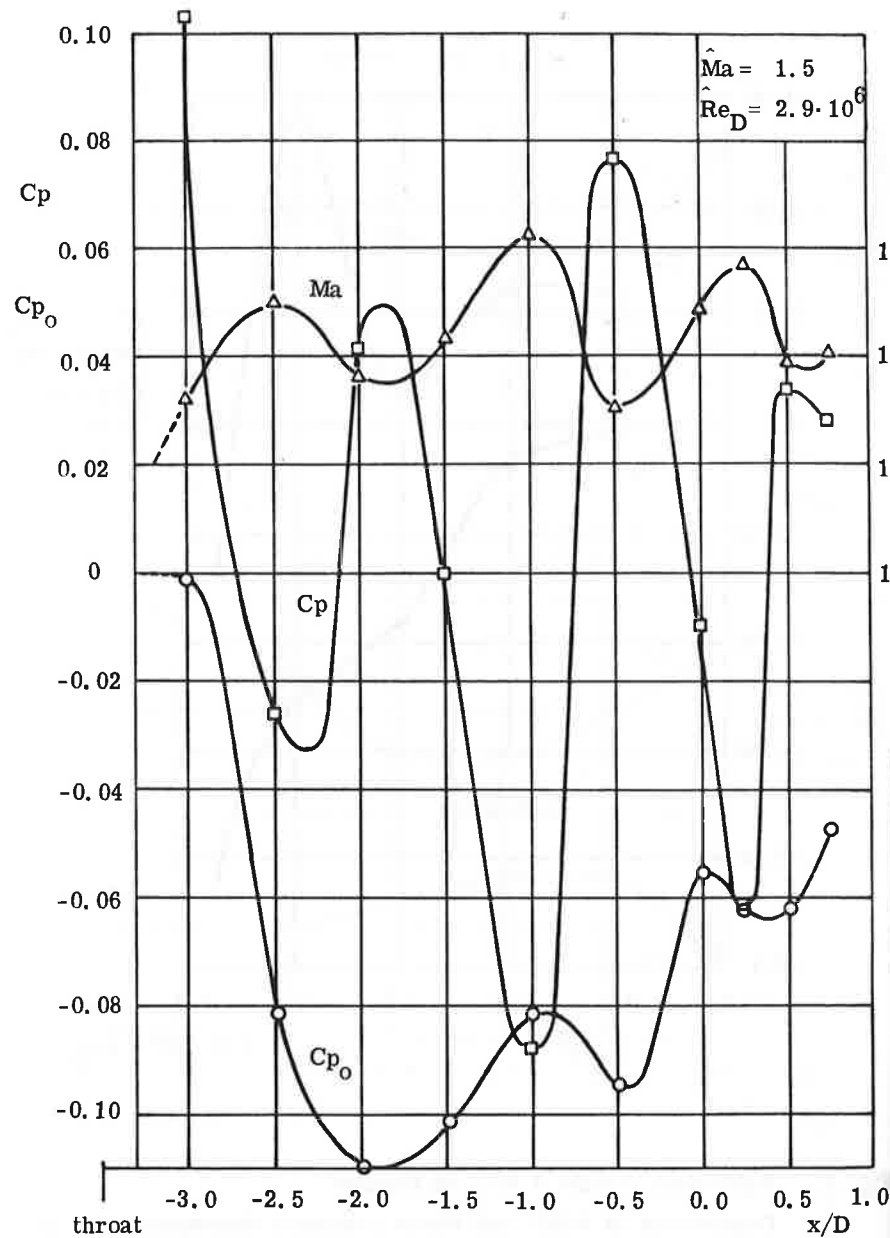


Fig. 9 Supersonic nozzle ϕ 80 / perforated
Total- and static pressure discrepancy coefficients and real Mach number along the axis

Fig. 10 shows for the contoured supersonic nozzle the total and static pressure discrepancy coefficients along the axis. The nozzle works at nominal operating conditions. Nominal means that the static pressure at the nozzle outlet is the same as ambient. The total pressure discrepancy coefficient could not be uniquely determined. The data lie within the dotted envelope. Surprising is the positive total pressure discrepancy coefficient for comparable cases. The static pressure discrepancy coefficient was shown to be repeatable.

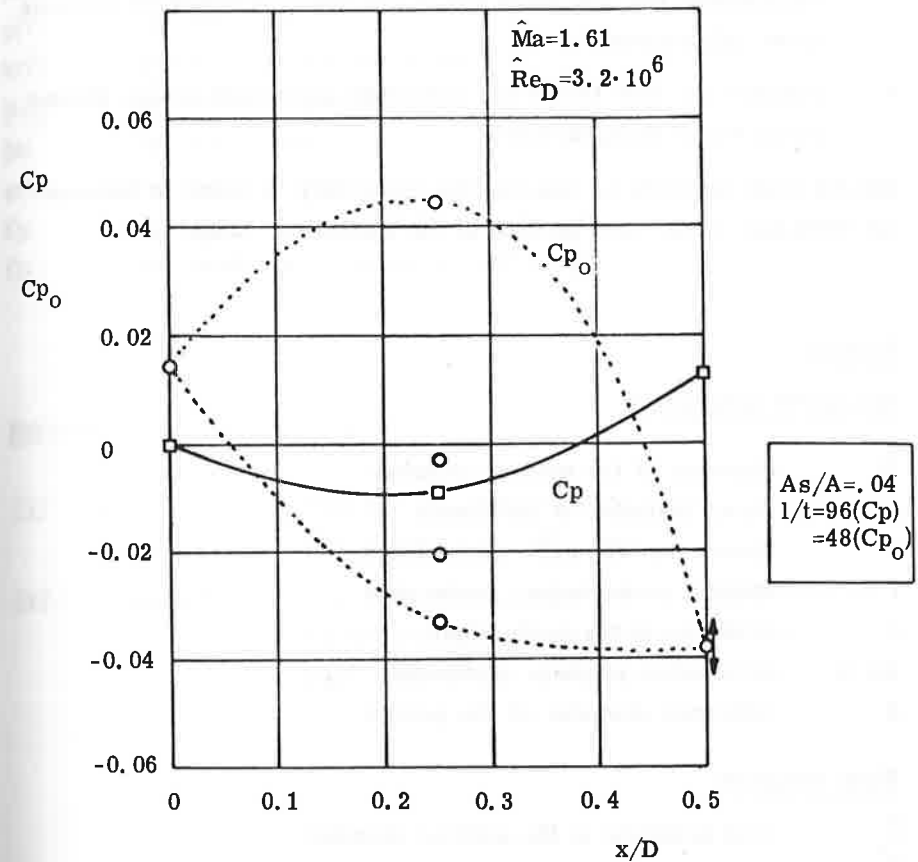


Fig. 10 Supersonic nozzle ϕ 80 / contoured
Total- and static pressure discrepancy coefficients along the axis

6. CONCLUSION

1. In the upper subsonic region a considerable probe-shaft influence was observed. Attention should be paid to the probe dimension and in particular to the shaft distance.
2. The flow behind the subsonic nozzles is more or less uniform. They are therefore suitable for probe calibrations.
3. The flow behind the perforated supersonic nozzle showed considerable non uniformity and is therefore unsuitable for accurate probe calibrations.
4. Similarly the flow behind the contoured supersonic nozzle showed considerable irregularities.

Efforts must be made to improve the uniformity in order to advance the technique of the flow probing in the supersonic range.

Notation

Geometric parameters

\hat{D}	diameter of the settling chamber
D	throat diameter of the nozzle
x	distance nozzle-exit / probe holes
l	distance probe holes / probe shaft
t	thickness of the probe shaft
As/A	probe shaft blockage coefficient
d	reference diameter of the probes

Flow variables

\hat{p}_0	total pressure in the settling chamber
\hat{T}_0	total temperature in the settling chamber
\hat{p}	ambient static pressure
\hat{T}	ideal static temperature

\hat{c}	ideal speed
$\nu(\hat{p}, \hat{T})$	ideal kinematic viscosity
p_0	total pressure in the test section
p	static pressure in the test section
T	real static temperature
c	real speed
$\nu(p, T)$	real kinematic viscosity
\hat{Re}_D	ideal Reynolds number
\hat{Ma}	ideal Mach number
$a(\hat{T})$	ideal speed of sound
$k(\hat{T})$	ideal ratio of specific heats
Re_D	real Reynolds number
Ma	real Mach number
$a(T)$	real speed of sound
C_p	static pressure discrepancy coefficient
C_{p_0}	total pressure discrepancy coefficient

References

- [1] Wille R.: Beiträge zur Phänomenologie der Freistrahlen DVL-Bericht Nr. 292 (1963)
- [2] Foelsch K.: The Analytical Design of an Axially Symmetric Laval Nozzle for a Parallel and Uniform Jet Journ. Aero. Sci., Vol. 16, No. 3 (1949)